

Vibrational modes of ^4He and H_2 gases adsorbed on carbon nanotubes

Silvina M. Gatica,^{1,*} Angela D. Lueking,^{2,3} Milton W. Cole,^{3,4} and Gerald D. Mahan^{3,4}

¹*Department of Physics and Astronomy, Howard University, 2355 Sixth Street, Northwest, Washington, DC 20059, USA*

²*Department of Energy and Mineral Engineering, Pennsylvania State University, University Park, Pennsylvania 16802-5000, USA*

³*Materials Research Institute, Pennsylvania State University, University Park, Pennsylvania 16802-5000, USA*

⁴*Department of Physics, Pennsylvania State University, University Park, Pennsylvania 16802-5000, USA*

(Received 12 April 2007; revised manuscript received 22 June 2007; published 7 August 2007)

We present calculations of the breathing mode phonon frequencies of ^4He and H_2 physically adsorbed on the outside surface of one or more carbon nanotubes. Two geometries are considered. The first is a single, isolated nanotube, upon which the gas is adsorbed as a commensurate phase. The second is a quasi-one-dimensional “groove” phase nestled between two nanotubes. While the computed breathing mode frequencies depend on nanotube radius and the adsorbate, in general, they are of the same order of magnitude as those of the bare nanotubes.

DOI: [10.1103/PhysRevB.76.085406](https://doi.org/10.1103/PhysRevB.76.085406)

PACS number(s): 68.43.Pq, 61.46.Fg, 63.22.+m, 68.49.Uv

I. INTRODUCTION

The problem of adsorbed phases of simple gases near carbon nanotubes has attracted much attention, due in part to the intriguing possibility of studying one-dimensional (1D) phases of matter and in part to potential applications, such as gas storage, sensing, and separation. Experimental techniques used to study such phases include scattering probes of structure,^{1,2} thermal probes of energies,³⁻⁵ and spectroscopic probes of the environment and dynamics of these films.⁶⁻⁸ Similar or identical techniques are also used to explore the bare nanotubes, or nanotube bundles, in order to elucidate their properties.⁹⁻¹¹ Compared to many surface science experimental systems, the traditional signal-to-noise problem of adsorption science is relatively less daunting for nanotubes because they are “all surface.”

In a recent paper,¹² denoted as Paper I, Lueking and Cole demonstrated interesting consequences of the fact that the curvature of nanotubes means that the separations between adsorption sites are larger than those between corresponding sites on the basal plane surface of graphite. As a result of this different geometry, distinctive commensurate phases on such nanotubes are expected to occur; these are thus far unobserved. The present paper addresses one way to study such phases, by measuring the frequency of long-wavelength phonon breathing modes. Such modes have been studied previously for bare nanotubes, and their spectrum can be related to the chirality of the tubes.^{13,14} In the present case, the measured spectrum can provide a stringent test of the theoretical adsorption potential, a subject of considerable interest in its own right because model potentials on nanotubes are often constructed from simple, but questionable, assumptions (such as pairwise additivity of interactions and transferability to nanotubes of empirical graphite interactions¹⁵). For specificity, the present calculations, like those of Paper I, are devoted exclusively to single-wall nanotubes (SWNTs); the generalization to multiwall cases is straightforward, in principle.

Section II of this paper derives the general relationship between the frequencies of the modes of the coupled gas-nanotube system and those derived for two simpler prob-

lems: the bare nanotube (ω_{NT}) and the adsorbed film vibrating near an assumed rigid substrate (ω_{AD}), respectively. There, it is shown that the mode frequencies of the coupled problem are numerically close in value to those of the two “simpler” problems. Section III presents computations of ω_{AD} for various gases in commensurate phases on single, isolated nanotubes. Section IV considers a different geometry, the “groove” phase situated between two tubes. That situation is present either at the external surface of a bundle of nanotubes or when a mat of close-packed, parallel nanotubes is laid out on a flat substrate surface. The calculations of the adsorbate spectrum are carried out for the quantum gases ^4He and H_2 . Similar calculations have been presented elsewhere (mostly for classical gases) in quasi-1D groove phases.^{16,17} Section V summarizes the principal results of this paper.

II. BREATHING MODES OF COUPLED ADSORBATE AND SUBSTRATE

Breathing modes are cylindrically symmetric oscillations of the nanotube and the adlayer. If one were to assume that the nanotube is rigid (as is usually assumed in studying films on graphite), the potential energy of the adlayer can be expanded in (assumed) small displacements about an equilibrium radial separation d_0 with a quadratic form having a force constant $k(R)$ that depends on the nanotube radius R . Adding to this energy is the energy associated with a hypothetical deviation of the value R from its equilibrium value, R_0 , that it would have in the absence of an adlayer. In the small amplitude approximation, this, too, is a quadratic form, with a force constant b . Adding to these fluctuation terms is the energy of the adlayer’s interaction with the nanotube, $V_0(R)$, resulting in the total energy, denoted $F(R, d)$:

$$F(R, d) = \frac{b}{2}(R - R_0)^2 + V_0(R) + \frac{k(R)}{2}[d - d_0(R)]^2. \quad (1)$$

Expanding all functions of R in a Taylor series about R_0 ,

$$F \approx \frac{b}{2}(R - R_0)^2 + V_0(R_0) + V'_0(R_0)(R - R_0) + \frac{V''_0}{2}(R - R_0)^2 + \frac{k(R_0)}{2}[d - d_0(R_0) - d'_0(R - R_0)]^2. \quad (2)$$

The classical equations of motion are

$$-M_{NT}\ddot{R} = \frac{\delta F}{\delta R} = V'_0 + k_R(R - R_0) - k_0 d'_0(d - d_0), \quad (3)$$

$$-M_{AL}\ddot{d} = \frac{\delta F}{\delta d} = k_0[d - d_0 - d'_0(R - R_0)], \quad (4)$$

where M_{NT} and M_{AL} are the nanotube and adlayer masses, respectively, $k_0 = k(R_0)$, $V_0 = V(R_0)$, and

$$k_R = b + V''_0 + k_0(d'_0)^2. \quad (5)$$

For oscillatory motion, assume a solution

$$-\ddot{R} = \omega^2(R - R_1) \equiv \omega^2 \delta R,$$

$$-\ddot{d} = \omega^2(d - d_1) \equiv \omega^2 \delta d,$$

where constants (R_1, d_1) need to be determined by the condition that all constant terms (i.e., not $\delta R, \delta d$) cancel,

$$M_{NT}\omega^2 \delta R - k_R \delta R + k_0 d'_0 \delta d = 0 = V'_0 + k_R(R_1 - R_0) - k_0 d'_0(d_1 - d_0),$$

$$M_{AL}\omega^2 \delta d - k_0 \delta d + k_0 d'_0 \delta R = 0 = k_0[d_1 - d_0 - d'_0(R_1 - R_0)].$$

Solving the right-hand side gives

$$R_1 - R_0 = -\frac{V'_0}{b + V''_0},$$

$$d_1 - d_0 = d'_0(R_1 - R_0) = -\frac{d'_0 V'_0}{b + V''_0}.$$

Solving the left-hand side gives

$$\omega^2 = \frac{1}{2} \left[\frac{k_R}{M_{NT}} + \frac{k_0}{M_{AL}} \pm \sqrt{\left(\frac{k_R}{M_{NT}} - \frac{k_0}{M_{AL}} \right)^2 + \frac{4k_0^2(d'_0)^2}{M_{NT}M_{AL}}} \right]. \quad (6)$$

We show below that the term involving the square of the derivative d'_0 is much less than 1. In this limit, the frequency spectrum has two frequencies that might be expected on intuitive grounds. One is $(k_R/M_{NT})^{1/2} = \omega_{NT}$. This is just the breathing mode frequency of a denuded nanotube. The second mode's frequency is $(k_0/M_{AL})^{1/2} = \omega_{AD}$, just what would be computed for an adlayer's vibration near a rigid nanotube. These results for the small d'_0 limit are completely analogous to the independent, decoupled vibrational and rotational frequencies of diatomic molecules when the vibration-rotation coupling is negligible.

The derivative of d_0 with respect to R is determined in the numerical calculations of the following section. The results are as follows: for H_2 , $d'_0 \sim 0.02$ for small radii NT where the

1×1 phase is stable to $d'_0 \sim 0.006$ for large radii NT where the $1 \times \sqrt{3}$ phase becomes stable. For ^4He , d'_0 is not a strong function of R , with a typical value $d'_0 \sim 0.016$. Under these circumstances, the coupling term, involving d'_0 , makes a small correction to the decoupled frequencies ω_{NT} and ω_{AD} (for both adsorbates). This correction may be evaluated by a small d'_0 expansion which yields

$$\omega_+ = \omega_{NT} + \Delta/\omega_{NT}, \quad (7)$$

$$\omega_- = \omega_{AL} - \Delta/\omega_{AL}. \quad (8)$$

The shift term is proportional to

$$\Delta = \frac{1}{2}(d'_0)^2(M_{AL}/M_{NT})\{\omega_{AL}^4/[\omega_{NT}^2 - \omega_{AL}^2]\}. \quad (9)$$

Since the frequencies and masses are comparable to one another, the quantity $(d'_0)^2$ determines the relative importance of this shift. Since $(d'_0)^2 \sim 10^{-4}$, the shift $(\omega_+ - \omega_{NT})$ of the “nanotube mode,” ω_+ , is small compared to ω_{NT} itself. We do note a rough proportionality of the shift Δ to the adlayer mass, which was found in recent experiments of Honda *et al.*¹⁸ In the following sections, because the correction is small, we proceed to compute the frequency of the adlayer mode (ω_-) by neglecting the correction term proportional to Δ ; that is, we take $\omega_- \sim \omega_{AD}$, equivalent to the assumption that the nanotubes are rigid.

III. BREATHING MODES OF ADSORBATE ON A SINGLE TUBE

The numerical method of Paper I was used to compute the adlayer angular frequency ω_{AD} for He and H_2 in commensurate phases on single, isolated nanotubes. In brief, the ground state potential energy V_{\min} for an adsorbed layer is computed for $(N, 0)$ zigzag SWNTs of various N , i.e., variable radius R . NT with radii in increments of $N=3$ were considered to accommodate the $\sqrt{3}$ phase. For each value of R , three possible commensurate phases were considered: the $\sqrt{3} \times \sqrt{3}$ $R30^\circ$ phase, the 1×1 phase, and a striped $1 \times \sqrt{3}$ phase. The last two phases are displayed in Fig. 1. The radii of the NTs considered here are in the range where the 1×1 phase is the most stable phase for He adsorption and either the 1×1 or the $1 \times \sqrt{3}$ phase is the most stable phase for H_2 adsorption (see Table I). The familiar $\sqrt{3} \times \sqrt{3}$ $R30^\circ$ stable phase is known to be the stable phase for He and H_2 on planar graphite, but higher density adlayers are accommodated on the tubes due to curvature, as described in Paper I. [Paper I indicates that the transition to the $\sqrt{3} \times \sqrt{3}$ $R30^\circ$ phase occurs for a (42,0) NT for H_2 adsorption and at radii greater than a (200,0) NT for He adsorption.] By investigating the dependence of the energy on the adsorbate distance d (Fig. 2) and minimizing, one obtains the equilibrium value (d_0) and the corresponding potential energy V_{\min} , tabulated below. Figures 3 and 4 display the dependence of d_0 on the radius of the tube for the most stable phases. The second derivative of the potential energy with respect to adlayer distance yields a breathing mode force constant, $k_0 = V''(d_0) = m\omega_{AD}^2$. The corresponding potential energy V_{\min} includes both adsorbate-adsorbate interactions and adsorbate-adsorbent interactions,

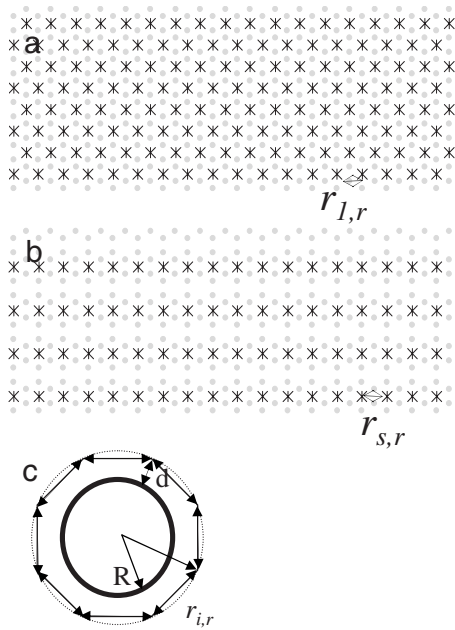


FIG. 1. [(a) and (b)] Nanotube projected onto two dimensions by unrolling the cylindrical graphite sheet. Adatoms (*) are arranged in (a) a 1×1 phase and (b) a striped $1 \times \sqrt{3}$ phase. (c) The transverse cross section shows the tube radius R , the equilibrium adsorption distance d , and radial atom nearest neighbor distance $r_{i,r}$.

as described in Paper I; in these calculations, the atomicity of the NT is important and the adsorbate-adsorbent interaction for each carbon atom is included in the ground state energy. In the table, we present an *estimate* of the total energy per adparticle:

TABLE I. Summary of stable phase parameters and breathing mode frequencies for commensurate phases on various SWNTs, with radius given. Note that the conversion from K to cm^{-1} is $1 \text{ K} \sim 0.695 \text{ cm}^{-1}$.

Radius (nm)	Stable phase	Eq. dist (Å)	V_{\min} (K)	$\hbar\omega_{AD}$ (K)	E_{est} (K)
Hydrogen					
0.23	1×1	2.78	-527	227	-413
0.35	1×1	2.82	-545	223	-434
0.47	$1 \times \sqrt{3}$	2.82	-516	231	-401
0.59	$1 \times \sqrt{3}$	2.84	-537	234	-420
0.70	$1 \times \sqrt{3}$	2.85	-552	234	-435
0.82	$1 \times \sqrt{3}$	2.85	-562	232	-446
Helium					
0.23	1×1	2.51	-166	101	-115
0.35	1×1	2.53	-181	105	-129
0.47	1×1	2.56	-189	104	-137
0.59	1×1	2.58	-193	101	-142
0.70	1×1	2.58	-195	105	-143
0.82	1×1	2.60	-196	100	-146

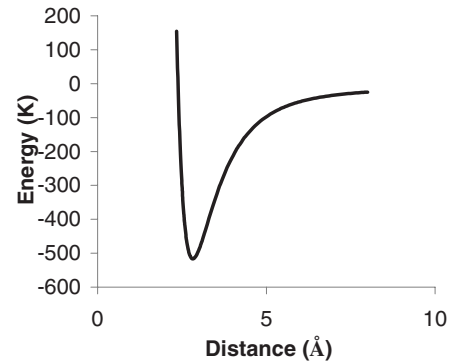


FIG. 2. H_2 -NT interaction for a $1 \times \sqrt{3}$ (stripe) phase adsorbed H_2 layer interacting with a (12,0) SWNT.

$$E_{\text{est}} = V_{\min} + \hbar\omega_{AD}/2. \quad (10)$$

The second term is the zero-point energy associated with the breathing mode; it is a significant energy, as discussed below. Omitted from this estimate is the contribution from circumferential quantum fluctuations, i.e., zero-point motions tangent to the nanotube. In an Einstein-like model, this “missing” energy would be $\hbar\omega_{CI}$, including two tangential degrees of freedom per particle, with an average frequency we call ω_{CI} . Although we have not calculated this energy, an estimate can be obtained from calculations and measurements carried out for helium and hydrogen films in commensurate phases on graphite;¹⁹⁻²¹ these results are $\hbar\omega_{CI} \sim 40 \text{ K}$ for hydrogen and $\hbar\omega_{CI} \sim 15 \text{ K}$ for helium, with an isotope dependence varying approximately as the inverse square root of the mass. These circumferential energy estimates are smaller than the tabulated radial frequencies: $\hbar\omega_{AD}$ is 220–230 K for H_2 and is $\sim 100 \text{ K}$ for a ^4He film adsorbed on a zigzag NT. These results are only slightly dependent on NT radii.

Note that the zero-point energy varies for H_2 , but not for He. This difference is likely due to a switch of the stable phase for H_2 in the range considered.

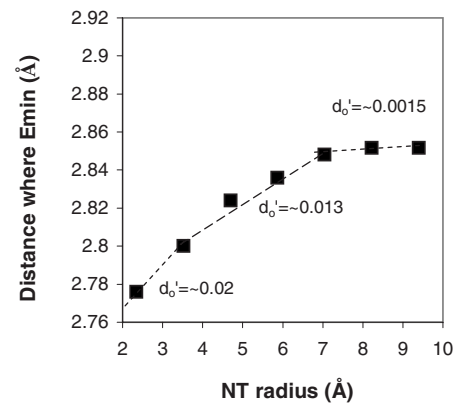


FIG. 3. Dependence of d_0 on R for H_2 adsorption. Values shown in the figure are for the striped phase, which is the most stable phase for NT with radii from 5 to 14 Å. The value of d_0' is a slowly varying function of radius, with the variation increasing at large radius.

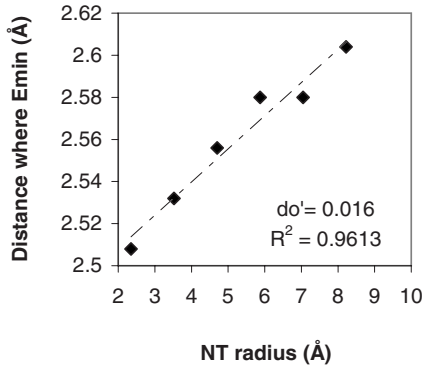


FIG. 4. Diamonds indicate the dependence of d_0 on R for He adsorption. Values shown in the figure are for the 1×1 phase, which is the most stable phase for the range of radius shown. The nearly straight line indicates that the value (~ 0.016) of d_0' is a weak function of radius, and one linear fit is shown.

For comparison with these breathing mode energies of the adlayer, we note that experimental measurements of energy levels of *single particles* near graphite have been obtained from bound state resonance (“selective adsorption”) energies deduced from molecular beam scattering data for graphite. The measured values for the ground state energy are -480 ± 5 K for H_2 and -144 ± 2 K for 4He .^{22,23} The corresponding vibrational excitation energies are 170 and 65 K, respectively. In comparing these graphite-derived values with the energies computed for a NT’s adlayer, there are several differences, having opposite effects, to consider. Two factors make the NT *less* attractive than graphite: (a) the nanotubes’ adsorption potential arises from a single surface, while the graphite potential has $\sim 30\%$ contribution from the semi-infinite subsurface layers, and (b) the nanotube surface is curved, reducing the attraction to some extent. The competing factor for the NT adlayer (increasing both its binding energy and the force constant) is that the adlayer’s breathing mode frequency includes the mutual interaction effects, which are considerable, compensating for the two factors mentioned above.

It is intriguing to observe that the total estimated energy for the NT adlayer is very similar (within 10%) to the ground state energy of a single 4He or H_2 molecule. In contrast, for both adsorbates, the adlayer breathing mode is significantly larger than that of a single particle; for example, in the H_2 case, the former is about 220 K while the latter is 170 K. We do not know why these quantities behave somewhat differently; the three environmental differences cited above, with competing signs, prevent us from offering a simple interpretation.

IV. MODES OF QUASI-1D FILM WITHIN A GROOVE

In this section, we evaluate the spectrum of transverse modes for the quantum gases He and H_2 confined in quasi-1D phases in the groove between two nanotubes. We take the z axis to lie parallel to the groove and the tubes’ axes, while the x axis is parallel to the vector between the center of one tube and that of the other nanotube. Similar

studies of this spectrum were carried out previously for other gases confined within the groove.^{16,17} As expected, there exist, in addition, longitudinal phonon modes (not studied here) propagating in the z direction, which are acoustic, with speeds determined primarily by the speed of sound of the (strictly) 1D phase, as determined by ground state calculations of these phases.^{24,25} The two branches of transverse modes occur at higher frequencies, arising when the ad-molecules vibrate perpendicular to the (z) direction of the groove. These modes are the focus of this section. In the specific circumstance considered here, the groove phase density ρ equals that (ρ_0) of the 1D equilibrium phase, so that the transverse mode frequencies at long wavelength are determined *solely* by the gas-surface interaction. The reason is that the transverse motion at this specific density affects the gas-gas interaction energy only to higher (quartic) order than the (gas-surface interaction) energy which enters the calculation of the phonon frequency. This fact means that the long-wavelength transverse frequencies are just those of an *independent* vibration of individual molecules in the groove. Because this statement would not be valid at finite wavelength, such modes would require a self-consistent phonon theory because of the large zero-point effects present for these highly quantum adsorbates. Such a self-consistent, quasi-1D theory, the analog of treatments of three-dimensional quantum solids, is beyond the scope of the present study. In any case, based on experience with other gases in this environment, we expect that the effect of the interparticle interaction on these modes is so small as to be negligible; the modes are essentially at constant frequency, independent of wavelength.

Because these modes of the groove phase are transverse and the potential energy in the groove is not cylindrically symmetric, the relevant spectrum involves two distinct frequencies. These are both determined from a single force constant for the film, called k_{NT} , which is evaluated from the substrate’s potential energy field. That field is the sum of contributions from the two tubes, which we assume to have identical radii R ; the more general case of distinct radii can be evaluated, if needed, from the adsorption potential of a single nanotube, $U(r)$, which is cylindrically symmetric. Lacking more detailed information about the chirality of the two nanotubes, we ignore discrete substrate atom effects on the potential and thus compute the frequencies from expressions derived previously for adsorption near a nanotube made of continuous carbon, i.e., smeared out atoms.^{16,17} The result in this case is that the two transverse mode frequencies satisfy

$$\omega_{Tx}(q) = (k_x/m)^{1/2}, \quad (11)$$

$$\omega_{Tz}(q) = (k_z/m)^{1/2}. \quad (12)$$

By analyzing the geometry of the groove phase, we deduce the force constant values from the interaction $U(r)$. Expanding this function about the minimum, at r_0 , one gets a force constant $k_{NT} = U''(r_0)$. Then, by analyzing the groove geometry, we get

$$k_x = 2k_{NT} \cos^2 \phi, \quad (13)$$

TABLE II. Values of $\Theta_{NT}=\hbar\omega_{NT}/k_B$ (in Kelvin) and ϕ (in parentheses, in radians) for He and H_2 in grooves with varying radii.

R (Å)	He	H_2
6	142 (0.496)	324 (0.541)
7	143 (0.470)	326 (0.513)
8	143 (0.447)	328 (0.489)

$$k_z = 2k_{NT} \sin^2 \phi. \quad (14)$$

Let us define $\omega_{NT}=(2k_{NT}/m)^{1/2}$. Then, $\omega_{Tx}(q)=\omega_{NT} \cos \phi$ and $\omega_{Tz}(q)=\omega_{NT} \sin \phi$. In these preceding expressions, the factor 2 arises from the additive contributions of the two nanotubes adjacent to the groove. ϕ is the angle between the line joining the tubes and the line from the center of a nanotube to the equilibrium position of the adatom. If the latter position lies at a height H above the plane containing the tubes' centers, and these centers are a distance d apart, then $\phi=\tan^{-1}(2H/d)=\cos^{-1}[d/(2r_{\min})]$, where r_{\min} is the equilibrium radial distance of the adsorbed particle above a *single* nanotube. Table II provides representative values of the various quantities, based on the assumption that $d=2R+3.35 \text{ \AA}$, the constant 3.35 \AA being the separation between the tubes.

These frequencies are approximately a factor 1.5 larger than those found for the geometry discussed in the previous section, a single nanotube. The principal reason for this difference is the fact that two nanotubes contribute to the restoring force in the groove case. That factor gives rise to a factor $2^{1/2}$ in the frequency, roughly the observed ratio of frequencies. This interpretation of the results is simple although both the mutual interactions and the atomicity of the

surface play a role in the single nanotube case, while they play no role in the groove phase.

V. SUMMARY

In this paper, we have computed the long-wavelength spectrum of breathing modes of the quantum gases ^4He and H_2 in two geometries. The contributions to these modes' frequencies arise from the substrate nanotubes, and these forces dominate the determination of the frequency explored here. The geometry of the first mode, discussed in Sec. III, is that of a commensurate phase adsorbed on a single nanotube. In that case, the mutual interactions between the adsorbed particles and the adsorption interaction contribute to the restoring force. The second geometry is that of a quasi-1D gas within the groove between two nanotubes. In that case, at the equilibrium density, the mutual interactions do not contribute to the restoring force because the long-wavelength motion changes no interparticle spacings.

The resulting frequencies in the groove phase are of order 140 K for ^4He and of 326 K for H_2 . They are a factor ~ 1.5 smaller for the commensurate phase on a single tube. The relationship between the results for the different geometries is attributed to the significantly stronger forces in the groove phase. The relationship between the frequency values for the two gases is qualitatively consistent with expectation based on the adsorption forces.

ACKNOWLEDGMENTS

This research has been supported by the National Science Foundation through Grants Nos. NSF-NIRT 0303916 and DMR-0505160. We are grateful to Peter Eklund for his suggestions and comments.

*Corresponding author; sgatica@howard.edu

¹M. R. Johnson, S. Rols, P. Wass, M. Muris, M. Bienfait, P. Zeppenfeld, and N. Dupont-Pavlovsky, *Chem. Phys.* **293**, 217 (2003).

²M. Bienfait, P. Zeppenfeld, N. Dupont-Pavlovsky, J.-P. Palmari, M. R. Johnson, T. Wilson, M. DePies, and O. E. Vilches, *Phys. Rev. Lett.* **91**, 035503 (2003).

³A. Kuznetsova, J. T. Yates, Jr., J. Liu, and R. E. Smalley, *J. Chem. Phys.* **112**, 9590 (2000); C. Matranga, *J. Phys. Chem. B* **107**, 12930 (2003); B. K. Pradhan, A. R. Harutyunyan, D. Stojkovic, J. C. Grossman, P. Zhang, M. W. Cole, V. Crespi, H. Goto, J. Fujiwara, and P. C. Eklund, *J. Mater. Res.* **17**, 2209 (2002); T. Ohba, K. Murata, K. Kaneko, W. A. Steele, F. Kokai, K. Takahashi, D. Kasuya, M. Yudasaka, and S. Iijima, *Nano Lett.* **1**, 371 (2001); A. C. Dillon and M. J. Heben, *Appl. Phys. A: Mater. Sci. Process.* **72**, 133 (2001).

⁴A. J. Zambano, S. Talapatra, and A. D. Migone, *Phys. Rev. B* **64**, 075415 (2001); S. Talapatra and A. D. Migone, *ibid.* **65**, 045416 (2002); A. J. Zambano, S. Talapatra, K. Lafdi, M. T. Aziz, W. McMillin, G. Shaughnessy, A. D. Migone, M. Yudasaka, S. Iijima, F. Kokai, and K. Takahashi, *Nanotechnology* **13**, 201

(2002); V. Krungleviciute, L. Heroux, A. D. Migone, C. T. Kingston, and B. Simard, *J. Phys. Chem. B* **109**, 9317 (2005).

⁵T. Wilson, A. Tyburski, M. R. DePies, O. E. Vilches, D. Becquet, and M. Bienfait, *J. Low Temp. Phys.* **126**, 403 (2002); T. Wilson and O. E. Vilches, *Low Temp. Phys.* **29**, 732 (2003); *Physica B* **329**, 278 (2003).

⁶Y. H. Kahng, R. B. Hallock, E. Dujardin, and T. W. Ebbesen, *J. Low Temp. Phys.* **126**, 223 (2003); J. C. Lasjaunias, K. Biljaković, J. L. Sauvajol, and P. Monceau, *Phys. Rev. Lett.* **91**, 025901 (2003).

⁷K. A. Williams, B. K. Pradhan, P. C. Eklund, M. K. Kostov, and M. W. Cole, *Phys. Rev. Lett.* **88**, 165502 (2002).

⁸D. G. Narehood, M. K. Kostov, P. C. Eklund, M. W. Cole, and P. E. Sokol, *Phys. Rev. B* **65**, 233401 (2002).

⁹S. Amelinckx, A. A. Lucas, and P. Lambin, *Rep. Prog. Phys.* **62**, 1471 (1999).

¹⁰M. S. Dresselhaus and P. C. Eklund, *Adv. Phys.* **49**, 705 (2000).

¹¹A. A. Lucas, F. Moreau, and Ph. Lambin, *Rev. Mod. Phys.* **74**, 1 (2002).

¹²A. D. Lueking and M. W. Cole, *Phys. Rev. B* **75**, 195425 (2007).

¹³S. Bandow, G. Chen, G. U. Sumanasekera, R. Gupta, M.

- Yudasaka, S. Iijima, and P. C. Eklund, *Phys. Rev. B* **66**, 075416 (2002); G. D. Mahan, *ibid.* **65**, 235402 (2002).
- ¹⁴R. B. Weisman, *Ind. Phys.* **10**, 24 (2004); A. Jorio, C. Fantini, M. A. Pimenta, D. A. Heller, M. S. Strano, M. S. Dresselhaus, Y. Oyama, J. Jiang, and R. Saito, *Appl. Phys. Lett.* **88**, 023109 (2006); J. Wu, W. Walukiewicz, W. Shan, E. Bourret-Courchesne, J. W. Ager III, K. M. Yu, E. E. Haller, K. Kissell, S. M. Bachilo, R. B. Weisman, and R. E. Smalley, *Phys. Rev. Lett.* **93**, 017404 (2004).
- ¹⁵See, e.g., M. K. Kostov, M. W. Cole, J. C. Lewis, P. Diep, and J. K. Johnson, *Chem. Phys. Lett.* **332**, 26 (2000).
- ¹⁶A. Šiber, *Phys. Rev. B* **66**, 205406 (2002); M. K. Kostov, M. M. Calbi, and M. W. Cole, *ibid.* **68**, 245403 (2003).
- ¹⁷M. T. Cvitaš and A. Šiber, *Phys. Rev. B* **67**, 193401 (2003).
- ¹⁸H. Honda, C.-M. Yang, H. Kanoh, H. Tanaka, T. Ohba, Y. Hattori, S. Utsumi, and K. Kaneko, *J. Phys. Chem. C* **111**, 3220 (2007).
- ¹⁹A. D. Novaco, *Phys. Rev. Lett.* **60**, 2058 (1988).
- ²⁰V. L. P. Frank, H. J. Lauter, and P. Leiderer, *Phys. Rev. Lett.* **61**, 436 (1988).
- ²¹J. M. Gottlieb and L. W. Bruch, *Phys. Rev. B* **41**, 7195 (1990).
- ²²L. Mattera, F. Rosatelli, C. Salvo, F. Tommasini, U. Valbusa, and G. Vidali, *Surf. Sci.* **93**, 515 (1980).
- ²³G. Boato, P. Cantini, R. Tatarek, and G. P. Felcher, *Surf. Sci.* **80**, 518 (1979); G. Derry, D. Wesner, W. E. Carlos, and D. R. Frankl, *ibid.* **87**, 629 (1979).
- ²⁴M. Boninsegni and S. Moroni, *J. Low Temp. Phys.* **118**, 1 (2000); E. Krotscheck, M. D. Miller, and J. Wojdylo, *Phys. Rev. B* **60**, 13028 (1999).
- ²⁵M. C. Gordillo, J. Boronat, and J. Casulleras, *Phys. Rev. B* **61**, R878 (2000); *Phys. Rev. Lett.* **85**, 2348 (2000); J. Boronat, M. C. Gordillo, and J. Casulleras, *J. Low Temp. Phys.* **126**, 199 (2002); L. Vranjes, Z. Antunovic, and S. Kilic, *Physica B* **349**, 408 (2004).